water

Article

Soil Infiltration Properties Are Affected by Typical Plant Communities in a Semi-Arid Desert Grassland in China

Shiling Shi [1,†], Feiyan Zhao [1,†], Xiaomeng Ren [2], Zhongju Meng [1,*], Xiaohong Dang [1] and Xiaolong Wu [1]

[1] College of Desert Control Science and Engineering, Inner Mongolia Agricultural University, Hohhot 010018, China
[2] Inner Mongolia Meteorological Institute, Hohhot 010051, China
* Correspondence: mengzhongju@126.com
† The authors contributed equally to this article.

Abstract: A process of infiltration from the soil surface to form soil water is known as soil infiltration; this is the only way for plants to absorb and use soil water. This process is closely related to nutrient migration, surface runoff, and soil erosion. The objectives of this study were to quantify the effect of typical plant communities on soil infiltration performance, reveal the interaction between soil infiltration rate and soil characteristics and plant roots, and determine the primary influencing elements on the Xilamuren grassland. The ring knife method was used to determine the soil infiltration rate at the 0–30 cm soil layer of six typical vegetation communities. The results indicated that the infiltration rate of the *Koeleria macrantha* community was highest at the soil depth of 0–5 cm, while that of the *Convolvulus ammannii* community was lowest, reaching 4.25 mm·min^{-1} and 0.53 mm·min^{-1}, respectively. The soil infiltration rate of different plant communities gradually declined with the increment of soil depth. The strongest correlations were found between bulk density, total porosity, organic matter, root characteristics, and soil infiltration rate. The bulk density, initial water content, capillary porosity, and clay content were the primary influencing factors acting on soil infiltration in the region. Other factors indirectly impacted the infiltration rate by modifying bulk density, which was a crucial limiting factor determining the infiltration rate in the research region. The study's findings will give theoretical and practical assistance for the prevention and management of soil deterioration and grassland restoration in this area.

Keywords: soil infiltration; plant community; root properties; semi-arid desert grassland

check for updates

Citation: Shi, S.; Zhao, F.; Ren, X.; Meng, Z.; Dang, X.; Wu, X. Soil Infiltration Properties Are Affected by Typical Plant Communities in a Semi-Arid Desert Grassland in China. *Water* **2022**, *14*, 3301. https://doi.org/10.3390/w14203301

Academic Editor: Roberto Greco

Received: 26 July 2022
Accepted: 17 October 2022
Published: 19 October 2022

1. Introduction

In recent years, global climate change and human disturbances such as overgrazing have affected the stability of the grassland ecosystems. In these landscapes, serious grassland degradation, plaque exposure, a high degree of surface compaction, and the formation of surface runoff have intensified soil erosion. Consequently, it is essential to explore the soil infiltration characteristics of degraded grasslands in semi-arid desert areas.

Soil water infiltration is the process of rainfall or irrigation water entering the soil vertically or horizontally through pores, connecting surface water, soil water, and groundwater [1]. This is an indispensable component of the hydrological cycle in terrestrial ecosystems [2]. There is an impact of both water supply and soil permeability on infiltration [2] that is strongly linked to overland runoff and soil erosion [3,4]. With strong soil infiltration capacity, rainfall penetrates the soil, effectively reducing surface runoff and soil erosion [5]. A lack of soil capacity to retain water and nutrients in arid regions is due to low precipitation, high evaporation, and low vegetation coverage. Plant growth and restoration in these areas are hampered by soil drought and barrenness. Infiltration of rainfall in the region is vital to soil water recharge, affecting grassland vegetation recovery, land degradation, and groundwater recharge [6]. Soil infiltration capability plays a critical role in enhancing soil water storage and retention. As an important soil hydrological parameter, soil permeability can be used as a key indicator to judge soil degradation and drought potential [7]. As a consequence, quantifying soil infiltration capability is extremely critical for regional ecological restoration [7].

Soil infiltration is a crucial physical property of soil moisture. It is now well established from a variety of studies that soil infiltration capacity is affected by a range of soil properties [8,9], and soil texture and structure are the basis for determining soil infiltration and hydraulic characteristics [10,11]. Water infiltration is governed by complex interactions between bulk density (BD), porosity, particle size distributions, organic matter (OM), water-stable aggregates, and soil water content [12,13]. In general, soils with coarser textures have higher permeability [14]. BD is primarily influenced by soil particle density and soil porosity, but it affects soil infiltration by changing soil porosity [15], and the soil infiltration rate (IR) is reduced with increasing soil BD [16]. It is unclear how soil organic matter content affects soil permeability, but the soil IR can vary with organic matter content [17].

There has been controversy surrounding the influence of biological soil crusts (BSCs) on soil infiltration. BSCs can hinder soil infiltration by blocking surface soil matrix pores and forming a relatively impervious layer [10,18]. The influence of biological crust thickness and soil particle size distribution will affect the impermeability of crusts [19]. In contrast, some other research results have demonstrated that BSCs can effectively improve soil water infiltration via rainfall interception, increasing surface roughness [20], improving soil structure, and promoting water absorption on surface soil [21,22]. Furthermore, according to Li et al. (2002) and Wang et al. (2007) [23,24], the effect of BSCs on infiltration capacity does not vary significantly, as they may be correlated with the comprehensive effects of rainfall intensity, soil type under the crust, and the vegetation in the region.

Soil water infiltration depends largely on plant properties. Recent research results have confirmed that soil infiltration is closely linked to above-ground biomass and plant litter [25] that affect soil infiltration by increasing surface roughness [26]. The high-density root network of plants improves the soil IR via altering the water infiltration capacity of the soil matrix [12,27,28]. Conversely, plant roots can reduce the soil infiltration capacity by clogging soil pores according to related research results [29,30]. The existing research focuses on using correlation and principal component analysis to examine the relationships between soil physicochemical properties, plant types, and soil water infiltration. Path analysis is rarely used to study soil infiltration characteristics under the condition of vegetation community change or to determine the main variables affecting soil infiltration.

Based on this, a great deal of previous research has concentrated on the effects of soil physical and chemical properties on soil infiltration. There has been little quantitative analysis of the relationship between soil infiltration characteristics of different plant communities, soil properties, plant types, and root structures in arid and semi-arid desert regions. This paper considers six typical vegetation communities in Xilamuren grassland in Inner Mongolia as the research object to (1) determine how soil properties, plant types, and root structure affect soil water infiltration in different plant communities; (2) identify factors affecting soil IR; and (3) reveal the main limiting factors affecting soil infiltration in the study area. It is hoped that these research findings will contribute to a deeper understanding of soil infiltration mechanisms and provide a scientific foundation for preventing grassland degradation and soil erosion in arid and semi-arid desert areas.

2. Material and Methods

2.1. Study Area

This study was conducted in the Xilamuren grassland of Damao Banner located in Inner Mongolia, China (Figure 1) (111°00′–111°20′ E, 41°12′–41°31′ N). The study area features a mid-temperate semi-arid continental monsoon climate. The rainfall is low throughout the year, with an average annual precipitation of 281 mm, mostly in the form of rainstorm (means short periods of high intensity rainfall) [7], and rainfall is unevenly distributed [31], occurring mainly in July and August. The main soil type is sandy loam;

the soil thickness is approximately 40–70 cm, and the lower soil has a high degree of calcification and a low content of soil humus. The natural vegetation belongs to the *Stipa grandis* community dominated by *Leymus chinensis* and *Stipa grandis*; other major plant species include perennial herbaceous plants such as *Artemisia frigida*, *Convolvulus ammannii*, and *Agropyron desertorum*, and the area has typical grassland features. The ecological environment is fragile in this region, as the area is located at the intersection of wind erosion and water erosion regions. The alternating effects of the two types of erosion lead to soil compaction and surface particle coarsening, and desert-type degradation is the primary manifestation of local grassland degradation. The experimental area was located in a closed pastoral area by the Institute of Water Resources for Pastoral Area. The terrain of the study area is relatively flat, eliminating human interference such as grazing and tourism, and the enclosed area measured 133 hm^2.

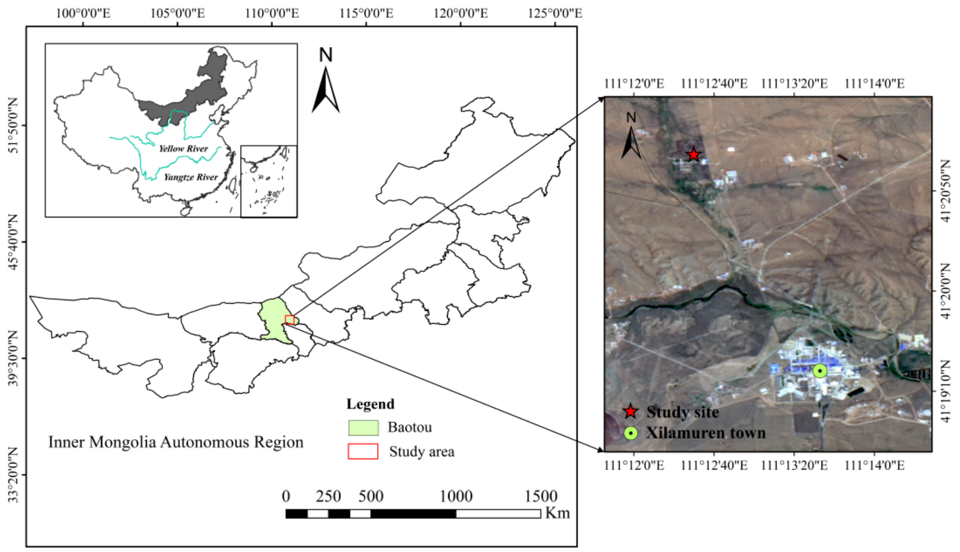

Figure 1. Location of the study site.

2.2. Experimental Design

The experiment was performed in the middle of August 2021 in the Xilamuren grassland in an enclosed area where there was no human disturbance. Four sample lines were arranged along the east–west direction; the distance between each sample line was 50 m, and the length of the sample lines was 300 m. Vegetation characteristics along the sample lines were investigated and recorded; 6–10 squares (1 m × 1 m) were set on each sample line according to the characteristics of plant communities and their dominant species. The study area comprised 35 plots where the height, coverage, abundance, and above-ground biomass of each plant were measured. Six typical community types of plots were selected by two-way indicator species analysis (TWINSPAN), and each type of plot contained 3–10 sample squares. The basic situation of the sample plots is shown in Table 1.

Table 1. Basic situations of the sampling plots.

Dominant Species	PSN	TC/%	AH/cm	AB/g	ST/cm	LB/g
AM + SG	9	45	25	187.07	30–40	78.70
CA	8	70	12	323.06	50–60	12.39
LC	18	80	30	341.48	50–60	96.94
KM + SG	20	95	35	532.18	60–70	114.67
SG	6	45	38	444.63	50–60	105.74
SB + SG	5	48	45	305.02	70–80	127.16

Note: Allium mongolicum + Stipa grandis (AM + SG), Convolvulus ammannii (CA), Leymus chinensis (LC), Koeleria macrantha + Stipa grandis (KM + SG), Stipa grandis (SG), Stipa breviflora + Stipa grandis (SB + SG); plant species number (PSN), total coverage (TC), average height (AH), above-ground biomass (AB), soil thickness (ST), and litter biomass (LB).

2.3. Collection and Determination of Soil Samples

The vertical profile of 0–30 cm soil was excavated in the selected sample plots, and we used a 100 cm^3 ring knife (width × height of 5 cm × 5 cm) to collect soil samples in four soil layers (0–5 cm, 5–10 cm, 10–20 cm, and 20–30 cm). The undisturbed soil structure was kept intact as much as possible in the sampling. The soil samples were placed in an aluminum box, immediately covered to avoid soil moisture evaporation, and weighed. The initial water content (IWC, %) and BD were measured by oven drying at 105 °C for 24 h to a constant weight (W_d). The soil particle size distributions were determined by a Malvern Mastersizer-3000 (Malvern Instruments Ltd., Malvern, UK). According to the soil texture classification method employed in China, the soil was divided into sand (1–0.05 mm), silt (0.05–0.002 mm) and clay (<0.002 mm). The OM content was determined by the dilution heat method. BD, total porosity (TP, %), capillary porosity (CP, %), and non-capillary porosity (NCP, %) were measured by the ring knife method. BD, TP, CP, and NCP were then calculated with the following formulae [32]:

(1) BD

$$\mathrm{BD}\left(\mathrm{g/cm^3}\right) = \frac{\mathrm{W_d} - \mathrm{W_c}}{\mathrm{V}}$$

where V is the ring knife volume (cm^3); W_c is the ring knife weight (g); and BD is the soil bulk density (g/cm^3).

(2) TP: Soil total porosity is generally not directly measured; rather, it is indirectly calculated by BD. The formula for soil TP was as follows [7]:

$$\mathrm{TP}\ (\%) = \left(1 - \frac{\mathrm{BD}}{ds}\right) \times 100$$

where *ds* is the soil particle density (2.65 g/cm^3 in this study).

(3) CP: Soil CP was measured by the ring knife method. The end of the obtained original ring knife soil sample with holes and filter paper was placed in a tray containing a thin layer of water. The water depth was maintained at 2–3 mm, and the soaking time was 8–12 h. If the soil sample inside the ring knife absorbed water and swelled, a knife was used to cut off the soil sample outside the ring knife, and the sample was immediately weighed. Water content was measured by oven drying at 105 °C for 24 h to a constant weight:

$$\mathrm{CP}\ (\%) = \frac{\mathrm{W_h}}{\mathrm{V}}$$

where V is the ring knife volume (cm^3), and W_h is the water content of the soil in the cutting ring after water absorption (g).

(4) NCP:

$$\mathrm{NCP}\ (\%) = \mathrm{TP} - \mathrm{CP}$$

2.4. Determination of Soil Infiltration Rate

The experiment was carried out in the laboratory of the Institute of Water Resources for the Pastoral Area. The soil IR was determined by the cutting ring (5 cm high, 100 cm^3). Undisturbed soils from 0–5 cm, 5–10 cm, 10–20 cm, and 20–30 cm layers of different community types were collected using cutting rings. To reduce marginal effects, Vaseline was applied inside the cutting rings before sampling to prevent water leakage at the edges during infiltration. Soil samples were taken back to the laboratory and soaked in distilled water for 12 h; the water depth was 5 cm, and the water level and ring knife mouth were kept flat. An empty ring cutter was docked over the cutting ring with undisturbed soil, and the gap between the two ring cutters was sealed with glass glue from the outside. The double-ring sampler was fixed after bonding with an iron frame. The ring edge was kept in the horizontal direction, and a funnel and beaker were placed under the soil to collect the water penetrating the soil. When the first drop of water dropped below the funnel, the beaker under the funnel was replaced every 2, 3, and 5 min according to the speed of water outflow, and the corresponding water leakage was measured.

During the experiment, water was added to maintain the water layer thickness at 5 cm, and the infiltration temperature was measured by a thermometer.

The measured IR K_0 was converted to the IR K_{10} at 10 °C using the following formula [33]:

$$K_{10} = K_\theta / (0.7 + 0.03 \times \theta)$$

where θ is the water temperature (°C), and K_θ is the IR (mm/min) when the water temperature is equal to θ.

(1) Calculation of soil initial infiltration rate (IIR) Since the reading error and systematic error in the initial observation phase cannot be estimated, the IIR f_0 (mm/min) was calculated as [34]:

$$f_0 = Q_0 / T_0$$

where Q_0 is the measured cumulative infiltration amount (mm) for 3 min from the beginning of infiltration, and T_0 is the time (3 min).

(2) Calculation of soil stable infiltration rate (SIR)

$$f_s = 0.510 \Delta h / \Delta t (0.7 + 0.03) T$$

where *fs* = soil SIR (mm/min) at 10 °C standard water temperature. Δh = water supply equipment reading difference (mm) in a certain period of time (Δt), and Δt is a certain period. T is the average water temperature during the period.

2.5. Determination of Plant Root System

After the soil infiltration experiment was completed, the soil in the ring knife was removed and rinsed in a 0.05 mm sieve until all the roots were washed out. The roots were put in an evaporating dish filled with distilled water and separated from the impurities with tweezers, and then, a root scanner was used for gray scanning. The Win RHIZO (Pro.2012b) software (Regent Instruments, Inc., Quebec City, Canada) was used to measure the parameters of total root length (TRL), root surface area (RSA), root average diameter (RAD), and root volume (RV). Finally, the roots were placed in a paper envelope and dried for 24 h at 65 °C to obtain root biomass (RB) [35].

For the convenience of comparative analysis, the data obtained in the experiment were the TRL, RSA, RAD, RV, and RB in the soil corresponding to the infiltration of the ring knife method.

2.6. Data Analysis

IBM SPSS 24.0 software (SPSS Inc., Chicago, IL, USA) were used to screen, calculate, and collate experimental data. One-way ANOVA and correlation analysis were used to investigate the differences in soil IR under different plant communities and to explore the correlation between soil IR and soil properties and plant root characteristics. Path analysis identified key environmental factors affecting soil infiltration in the Xilamuren grassland.

3. Results

3.1. Soil Infiltration Properties under Different Plant Communities

The soil IIR and SIR of different communities under different soil layers were the same (Figures 2 and 3). In general, the soil IRs of all plant communities except *Allium mongolicum*, *Convolvulus ammannii*, and the *Stipa grandis* community decreased with increasing soil depth. Meanwhile, the IRs of different communities had large differences among different soil layers. The difference in IR among different communities was most significant in the 0–5 cm soil depth layer. The IIR and SIR of the *Koeleria macrantha* community were higher than those of other communities ($p < 0.05$), reaching 4.25 mm/min and 2.71 mm/min, respectively, which is followed by the *Stipa breviflora* community, where the IIR and SIR were 3.5 mm/min and 1.97 mm/min, respectively. The IR of the *Convolvulus ammannii* community was significantly lower than those of other plant communities; the IIR and SIR values were 0.53 mm/min and 0.29 mm/min, respectively: only 10% and 12% of the IIR and SIR values of the *Koeleria macrantha* community ($p < 0.05$). The difference in IR gradually declined with the soil depth among different plant communities. At the depth layer of 5–10 cm, the IIR and SIR of *Koeleria macrantha* were significantly higher than those of the *Stipa breviflora* community ($p < 0.05$). The *Convolvulus ammannii* and *Koeleria macrantha* communities at the layer of 10–20 cm soil showed the greatest IIR, but the *Stipa grandis* community at the depth of 20–30 cm showed the greatest SIR ($p < 0.05$). The IIR of different plant communities at depth of the 20–30 cm had no significant differences ($p > 0.05$).

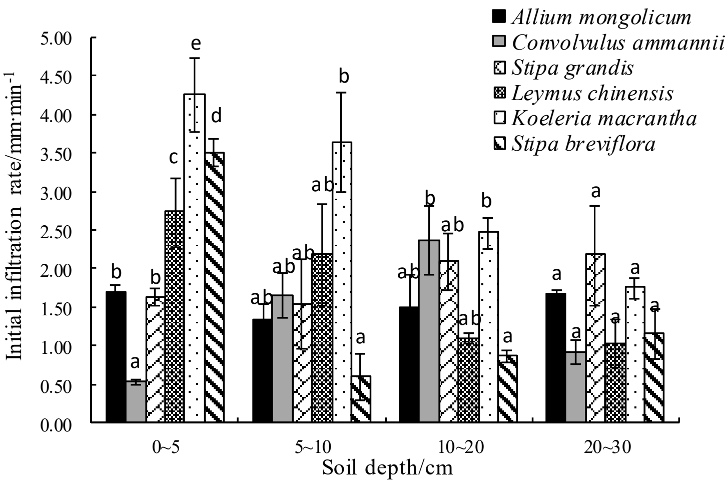

Figure 2. Soil IIR under different vegetation communities. Note: different letters (a,b,c,d,e) indicate significant differences ($p < 0.05$) among different plant communities.

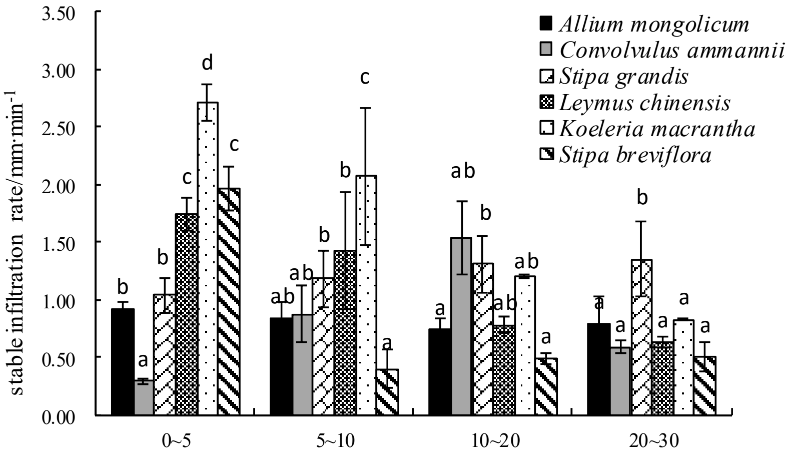

Figure 3. Soil SIR under different vegetation communities. Note: different letters (a,b,c,d) indicate significant differences ($p < 0.05$) among different plant communities.

3.2. Relationship between Soil Infiltration Properties and Environmental Factors

The soil characteristics and root properties of natural grasslands varied considerably with plant communities and soil depth layers (Tables 2 and 3). The soil BD, porosity, and OM content had a certain regularity between different soil layers. The BD of different plant communities ranged from 1.16 to 1.69 g/cm^3. The BD in each plant community increased with increasing soil depth, and the TP, CP, and OM decreased with increasing soil depth layers in each plant community except for the *Convolvulus ammannii* community. However, the IWC and NCP of different plant communities had no clear regularity with increasing soil depth. In terms of soil texture, the *Allium mongolicum* community showed higher sand content (SC) and lower silt content (SIC) in different soil layers, being 69.97% and 29.91%, respectively, while the *Stipa breviflora* community showed lower SC and the greatest SIC in each soil depth layer, at 41.19% and 58.40%, respectively. Plant roots of different communities were concentrated at the depth of 0–5 cm. As soil depth increased, the amount of vegetation roots dwindled. The grass roots of the *Koeleria macrantha* community were more developed; among the six community plots, the *Convolvulus ammannii* community had the most sparse plant root system (Table 3).

Table 2. Soil characteristics of different communities.

VT	SD (cm)	BD (g/cm^3)	IWC (%)	TP (%)	CP (%)	NCP (%)	OM (g/kg)	Particle Size Composition		
								CC (%)	SIC (%)	SC (%)
AM	0–5 cm	1.48	6.88	44.15	38.36	6.81	14.46	0.19	34.08	65.73
	5–10 cm	1.42	7.75	46.42	41.91	5.24	10.59	0.08	19.79	80.13
	10–20 cm	1.48	6.60	44.15	39.66	5.52	12.11	0.10	33.90	66.00
	20–30 cm	1.55	6.03	41.51	36.95	5.92	12.29	0.09	31.88	68.02
CA	0–5 cm	1.60	7.52	39.62	36.52	4.70	12.86	0.12	41.97	57.91
	5–10 cm	1.59	6.18	40.00	36.47	5.08	9.90	0.25	35.71	64.04
	10–20 cm	1.52	5.17	42.64	37.51	6.34	9.28	0.13	39.02	60.85
	20–30 cm	1.58	5.85	40.38	36.23	5.65	9.80	0.46	50.58	48.96
SG	0–5 cm	1.38	6.96	47.92	43.20	5.27	18.58	0.59	62.56	36.85
	5–10 cm	1.48	6.65	44.15	38.28	6.89	12.57	0.17	27.59	72.24
	10–20 cm	1.59	5.08	40.00	34.64	6.91	9.06	0.06	15.53	84.41
	20–30 cm	1.67	4.03	36.98	31.80	7.11	9.01	0.03	14.14	85.83
LC	0–5 cm	1.27	7.84	52.08	45.02	7.07	21.86	0.67	57.38	41.96
	5–10 cm	1.31	8.15	50.57	44.46	6.31	13.87	0.53	53.48	45.99
	10–20 cm	1.45	8.58	45.28	39.50	6.66	12.28	0.18	37.87	61.95
	20–30 cm	1.58	6.88	40.38	35.57	6.31	9.94	0.23	28.44	71.33
KM	0–5 cm	1.16	7.19	56.23	47.70	8.02	23.59	0.97	63.35	35.68
	5–10 cm	1.22	7.58	53.96	45.56	8.18	24.58	0.83	53.64	45.53
	10–20 cm	1.43	7.61	46.04	39.04	7.78	17.58	0.26	30.31	69.44
	20–30 cm	1.54	6.88	41.89	37.45	5.75	15.28	0.42	34.01	65.57
SB	0–5 cm	1.31	7.62	50.57	42.47	8.31	17.00	0.78	68.40	30.82
	5–10 cm	1.43	7.95	46.04	38.96	7.87	12.56	0.26	50.77	48.97
	10–20 cm	1.63	8.99	38.49	35.00	5.23	12.25	0.28	53.70	46.02
	20–30 cm	1.69	8.55	36.23	32.19	6.07	10.18	0.33	60.74	38.93

Note: vegetation type (VT), soil depth (SD), bulk density (BD), initial water content (IWC), total porosity (TP), capillary porosity (CP), non-capillary porosity (NCP), organic matter (OM), clay content (CC), silt content (SIC), sand content (SC); *Allium mongolicum* (AM), *Convolvulus ammannii* (CA), *Stipa grandis* (SG), *Leymus chinensis* (LC), *Koeleria macrantha* (KM), and *Stipa breviflora* (SB).

Soil infiltration was intimately linked to soil particle size composition. The IWC and SC showed negative correlations with soil IR; the RAD of plants was positively correlated with IR, although the correlation was not significant (Table 4). Other soil properties and plant root indices were highly significantly correlated with IIR and SIR. The influence of BD on soil infiltration was the opposite and was markedly negatively related to IIR and SIR ($p < 0.01$). The TP was significantly positively correlated with IIR and SIR, the same as the soil BD ($p < 0.01$). The TP was calculated from the soil BD in this study, so the correlation coefficient between these two parameters was the same. The correlation between SC and IIR and SIR was relatively low compared with other indices. Meanwhile, it could also be seen from the correlation between various environmental factors that in addition to the IWC, the correlations between soil properties and the characteristics of plant roots generally reached a significant level ($p < 0.05$), and soil BD and SC were significantly negatively correlated with each index of the plant root system ($p < 0.05$). The BD, CP, and OM contents were extremely significantly correlated with other environmental factors ($p < 0.01$), indicating that plant community types and soil environmental factors in different soil layers affected the soil infiltration process, and there were significant interactions (Table 4). A simple correlation analysis can only reflect the closeness of a connection. Therefore, we decided to further use path analysis to determine the direct and indirect importance of the independent variables to the dependent variables.

Table 3. Root characteristics of different communities.

VT	SD (cm)	TRL (cm)	RSA (cm^2)	RAD (mm)	RV (cm^3)	RB (g)
AM	0–5 cm	405.42	103.66	0.81	2.11	1.20
	5–10 cm	413.47	50.62	0.39	0.49	0.29
	10–20 cm	264.81	30.51	0.37	0.28	0.15
	20–30 cm	109.67	14.20	0.37	0.22	0.06
CA	0–5 cm	232.59	62.58	0.87	1.25	0.91
	5–10 cm	192.58	43.76	0.55	0.60	0.31
	10–20 cm	105.34	11.71	0.35	0.10	0.06
	20–30 cm	42.26	4.32	0.32	0.04	0.02
SG	0–5 cm	480.73	110.66	0.73	2.06	1.18
	5–10 cm	255.23	32.25	0.40	0.62	0.29
	10–20 cm	267.84	28.78	0.34	0.25	0.14
	20–30 cm	176.43	19.46	0.35	0.17	0.10
LC	0–5 cm	394.39	121.79	0.71	1.96	1.18
	5–10 cm	314.23	63.55	0.64	1.02	0.59
	10–20 cm	82.73	14.79	0.57	0.21	0.18
	20–30 cm	42.29	7.58	0.57	0.11	0.07
KM	0–5 cm	543.85	281.32	1.25	6.51	2.62
	5–10 cm	416.43	61.22	0.39	2.5	1.29
	10–20 cm	267.72	28.78	0.34	0.25	0.15
	20–30 cm	177.37	19.51	0.35	0.17	0.10
SB	0–5 cm	301.55	81.83	0.71	1.87	1.04
	5–10 cm	162.85	22.94	0.44	0.47	0.20
	10–20 cm	194.49	18.19	0.62	0.50	0.21
	20–30 cm	117.17	18.82	0.42	0.20	0.07

Note: vegetation type (VT), soil depth (SD), total root length(TRL), root surface-area (RSA), root average diameter (RAD), root volume (RV), root biomass (RB); *Allium mongolicum* (AM), *Convolvulus ammannii* (CA), *Stipa grandis* (SG), *Leymus chinensis* (LC), *Koeleria macrantha* (KM), and *Stipa breviflora* (SB).

Table 4. Correlation analysis between infiltration rate and environmental factors.

	BD	IWC	TP	CP	NCP	OM	CC	SIC	SC	TRL	RSA	RAD	RV	RB
BD	1.000													
IWC	−0.333	1.000												
TP	−1.00	0.335	1.000											
CP	−0.978 **	0.370	0.978 **	1.000										
NCP	−0.565 **	0.024	0.565 **	0.379	1.000									
OM	−0.843**	0.368	0.843 **	0.816 **	0.508 **	1.000								
CC	−0.762 **	0.348	0.762 **	0.738 **	0.457 *	0.827 **	1.000							
SIC	−0.494 **	0.558 **	0.494 *	0.507 *	0.186	0.567 **	0.800 **	1.000						
SC	0.500 **	−0.557 **	−0.500 *	−0.512 **	−0.192	−0.573 **	−0.806 **	−1.000	1.000					
TRL	−0.724 **	0.151	0.724 **	0.722 **	0.352	0.785 **	0.612 **	−1.000	−0.368	1.000				
RSA	−0.701 **	0.156	0.701 **	0.705 **	0.320	0.710 **	0.677 **	0.363	−0.475 *	0.834 **	1.000			
RAD	−0.487 *	0.343	0.487 *	0.518 **	0.109	0.530 **	0.542 **	0.470 *	−0.538 **	0.627 **	0.856 **	1.000		
RV	−0.726 **	0.176	0.726 **	0.710 **	0.407 *	0.767 **	0.746 **	0.536 **	−0.527 **	0.815 **	0.967 **	0.821 **	1.000	
RB	−0.747 **	0.214	0.747 **	0.742 **	0.373	0.804 **	0.750 **	0.521 **	−0.553 **	0.866 **	0.953 **	0.849 **	0.977 **	1.000
IIR	−0.729 **	−0.321	0.729 **	0.641 **	0.693 **	0.706 **	0.684 **	0.548 **	−0.292	0.651 **	0.637 **	0.323	0.686 **	0.659 **
SIR	−0.741 **	−0.327	0.741 **	0.657 **	0.682 **	0.684 **	0.679 **	0.585 **	−0.278	0.659 **	0.664 **	0.355	0.700 **	0.669 **

Note: bulk density (BD), initial water content (IWC), total porosity (TP), capillary porosity (CP), non-capillary porosity (NCP), organic matter (OM), clay content (CC), silt content (SIC), sand content (SC), total root length (TRL), root surface-area (RSA), roots average diameter (RAD), root volume (RV), root biomass (RB), initial infiltration rate (IIR), and stable infiltration rate (SIR). * Represents significant correlation at the $p < 0.05$ level. ** represents significant correlation at the $p < 0.01$ level.

3.3. Influence Mechanism of Soil Infiltration

A total of 24 different samples were selected for this test. First, a normality test was performed on the dependent variables (IIR and SIR). After that, the soil IIR and SIR were selected as the dependent variables Y_1 and Y_2, and the following 13 factors were selected as the independent factors: SD (X_1), IWC (X_2), CP (X_3), NCP (X_4), OM (X_5), CC (X_6), SIC (X_7), SC (X_8), TRL (X_9), RSA (X_{10}), RAD (X_{11}), RV (X_{12}), and RB (X_{13}). Multivariate stepwise regression was used to screen out relatively independent and important influencing factors affecting soil initial and stable IRs. A path analysis was further performed to determine their relationships to the extent of soil infiltration (Table 5).

The values of the Shapiro–Wilk statistics for soil IIR and SIR were 0.919 and 0.934 (Table 5), and the significance level was greater than 0.05 in both cases (p = 0.054 and p = 0.120). Therefore, the distributions of dependent variables were not significantly different from normal distributions.

The regression equations were as follows:

$$Y_1 = 31.294 - 11.634X_1 - 0.315X_2 + 0.271X_3 + 1.341X_6$$

$$Y_2 = 18.577 - 6.997X_1 - 0.202X_2 + 0.154X_3 + 0.768X_6$$

After inspection and analysis, the R^2 values of soil IIR and SIR were 0.81 and 0.85, respectively; there was a significant difference between the independent and dependent variables, and the equation was statistically significant. Meanwhile, the multiple regression equation showed that soil BD, IWC, CP, and CC were the crucial factors affecting soil IR in the study area.

The direction and magnitude of the direct and indirect effects of the main environmental factors on soil IIR are listed in Table 6. The absolute values of the direct path coefficients of soil IIR and related factors in the study area from large to small were BD > CP > IWC > CC. Among these, the direct path coefficient of BD was −1.737, indicating that BD had the strongest direct negative impact on the IIR. This indicated that soil BD was the main limiting factor, and its indirect effects on soil IIR via CP and CC were negative. The direct positive effect of CC on soil IIR was weak (0.376), but the indirect positive effects of BD, IWC, and CP on soil IIR were the largest (2.063). The positive and negative path coefficients indicated that the independent variables promoted and inhibited the response variables, indicating that soil BD and IWC had an inhibitory effect on the IIR.

The absolute values of the direct path coefficients of the SIR and the related factors in the study area from high to low were BD > CP > IWC > CC (Table 7). The size of soil BD was directly correlated with soil porosity and soil water conductivity rate. Therefore, the direct path coefficient of soil SIR was −1.674, which was greater than other indirect path coefficients. Soil SIR was strongly influenced by CP, and it had an indirect effect on soil SIR via BD and CC. The direct effect of soil IWC and CC on soil SIR was weak, affecting soil SIR via soil BD and CP.

Table 5. Regression equation of infiltration rate and environmental factors.

	Kolmogorov–Smirnova			Shapiro–Wilk			Stepwise Multiple Regression Equation	R^2
	Statistics	***df***	***p***	**Statistics**	***df***	***p***		
Initial Infiltration Rate	0.166	24	0.086	0.919	24	0.054	$Y_1 = 31.294 - 11.634X_1 - 0.315X_2 + 0.271X_3 + 1.341X_6$	0.81
Stable Infiltration Rate	0.131	24	0.200 *	0.934	24	0.120	$Y_2 = 18.577 - 6.997X_1 - 0.202X_2 + 0.154X_3 + 0.768X_6$	0.85

Note: * Represents significant correlation at the $p < 0.05$ level.

Table 6. Path coefficient between environmental factors and soil IIR.

Independent Variable	Correlation Coefficient	Direct Path Coefficient	Indirect Path Coefficients					Decision Coefficient
			BD	IWC	CP	CC	Total	
BD	0.729	−1.737		0.135	−1.164	−0.286	−1.316	−5.547
IWC	−0.123	−0.397	0.590		0.440	0.278	1.309	−0.060
CP	0.641	1.188	1.702	−0.147		0.278	1.834	0.111
CC	0.684	0.376	1.320	−0.139	0.879		2.063	0.374

Note: bulk density (BD), initial water content (IWC), capillary porosity (CP), and clay content (CC).

Table 7. Path coefficient between environmental factors and soil SIR.

Independent Variable	Correlation Coefficient	Direct Path Coefficient	Indirect Path Coefficients					Decision Coefficient
			BD	IWC	CP	CC	Total	
BD	0.741	−1.674		0.139	−1.061	−0.262	−1.185	−5.284
IWC	−0.127	−0.408	0.569		0.401	0.255	1.225	−0.062
CP	0.657	1.083	1.641	−0.151		0.255	1.745	0.251
CC	0.679	0.345	1.272	−0.143	0.801		1.931	0.350

Note: bulk density (BD), initial water content (IWC), capillary porosity (CP), and clay content (CC).

4. Discussion

4.1. Soil Infiltration Properties under Different Plant Communities

Soil infiltration is the process of water flowing through the earth's surface and infiltrating the soil to form soil water. This is the main way for plants to absorb and use soil moisture [36]. There are large differences in soil permeability characteristics between different vegetation types, different restoration stages, and different soil thicknesses [14,27,37]. According to the current study, plant communities and soil thickness significantly affected soil infiltration properties (Figures 2 and 3). Conversely, it was reported by Hu et al. (2009) [38] that the vegetation community type had little impact on soil IR. These differences may be accounted for by differences in the soil and plant properties of various vegetation communities [39,40]. As shown above, our research discovered that the soil properties and root characteristics of natural grassland are different among plant communities and soil depth layers (Tables 2 and 3). Kalhoro et al. (2019) [41] demonstrated that with increasing depth in the soil profile, the saturated hydraulic conductivity of different vegetation succession stages decreased; our research also found the same result except for the *Convolvulus ammannii* community and the *Stipa grandis* community. The soil compactness and porosity depend on the soil BD and porosity [2]. Generally, soil porosity declined with the deeper soil layers; BD increased, and thus, soil IR decreased (Table 2). The soil IIR and SIR of the *Koeleria macrantha* community at the 0–10 cm soil depth were considerably higher than those of the other communities. According to the field survey, the *Koeleria macrantha* community had high total coverage and above-ground biomass (Table 1), was rich in surface litter content, and had a thick humus layer. In addition, it had a rich root network that effectively improved the soil structure and was beneficial to soil infiltration. The SC of the *Stipa grandis* community at the 10–30 cm soil layer was higher, and the soil porosity between particles was larger, so the soil IR was higher (Table 2; Figures 2 and 3). There was also serious plant degradation of the *Convolvulus ammannii* community in the field investigation. Raindrop splash erosion was obvious during the rainfall; in addition, the surface appeared to have bare patches and was severely compacted. This hindered water infiltration, and thus, the IR of the 0–5 cm soil layer was relatively low (Table 1; Figures 2 and 3).

4.2. Factors Influencing Infiltration Properties

Soil water infiltration is a complex hydrological process, and it is an important part of evaluating the water regulation capacity of vegetation layers [42]. Typically, it has been found that soil infiltration capacity is generally controlled by both soil properties and plant characteristics such as BD, IWC, OM, soil porosity, and plant roots [7,30]. Correlation and path analyses were performed to clarify the degree of influence of soil properties and plant characteristics on IR. We found that the soil infiltration level in Xilamuren grassland was significantly correlated with other soil properties (BD, TP, CP, NCP, soil particle size composition, and OM; see Table 4). This result was consistent with the findings of Benavides et al. (2018) [43] and Azooz et al. (1996) [44]. According to the results from Zhu et al. (2020) [12], soils with higher CC generally have lower BD, and the impacts on IR are due to the particle size being smaller, resulting in smaller spaces between particles that in turn reduce hydraulic conductivity and IR. Moreover, the CP was significantly positively correlated with soil IR. As Kabir et al. (2020) [37] reported, soil permeability is increased by enhancing capillary and gravitational forces. Meanwhile, previous research has also demonstrated that soil IWC has an impact on soil infiltration by affecting the rate of water diffusion in the soil [45]. Our study found that the IWC was negatively correlated with IIR and SIR, but the correlations were weak. This phenomenon may be due to the study plot experiencing perennial drought and less rain; the soil IWC was much lower than the field water-holding rate. The soil samples were saturated with water before determination, weakening the effect of soil water suction on IR. This may also have been due to the difference in plant community water use or shading from above-ground biomass being different due to the plant community etc. Moreover, the higher soil IWC may lead to the greater swelling of clay particles in the soil, causing reductions in the soil pores and hydraulic gradient. The IIR and SIR are reduced under the higher IWC [46].

Soil IIR and SIR are also influenced by plant roots. Plant root properties such as TRL, RSA, RAD, RV, and RB were significantly correlated with IIR and SIR in our study [47–49]. Cui et al. (2019) [6] pointed out that the RAD of different plants has significant differences among different infiltration stages. Here, there was a significantly positive correlation between 0–2 mm RAD and soil IR; the 2–4.5 mm RAD was weakly correlated with IR, and RAD greater than 4.5 mm was negatively correlated with permeability. In our study, the RAD of different vegetation communities was less than 2 mm (Table 3). The growth and decomposition of plant roots can accelerate soil IR [50,51]. Root residues are a crucial source of carbon supplementation in the soil, as they can increase soil OM, promote the formation of soil aggregates, and change the soil structure, thus being conducive to soil infiltration [6,48,52]. Our study revealed that the soil root index was significantly positively correlated with OM. In addition, many studies have reported an interaction between the soil and root system that can change the soil aggregate structure via root exudates, interspersed extrusion, and entanglement of fibrous roots [53–55], thus affecting soil IR.

Path analysis indicated that soil BD, IWC, CP, and CC had direct or indirect effects on soil IIR and SIR (Tables 6 and 7). Soil BD was the major limiting factor affecting soil IR, as it could reduce the hindrance to water infiltration by changing soil porosity and texture. The indirect promoting impact of CC on soil IIR and SIR was considerably greater than the direct effect. Soil CP positively contributed to soil IIR and SIR and indirectly affected soil IR by altering soil BD and CC. This may have been due to the high degree of surface compaction, high CC and lower soil porosity in the study area, which are factors that reduced the soil infiltration capacity. The IWC of the study area was indirectly influenced on soil IR by soil BD and CP, indicating that soil BD and CP had different effects on soil infiltration under different water content conditions. Lipiec et al. (2006) [56] drew similar conclusions. Overall, the soil infiltration characteristics of Xilamuren grassland were primarily affected by soil BD, IWC, CP, and soil texture (CC).

5. Conclusions

In the Xilamuren grassland, the soil IIR and SIR differed significantly between different plant communities. The IR was the highest in the *Koeleria macrantha* community and the lowest in the *Convolvulus ammannii* community, and the IR of each community decreased with the increasing soil depth. Soil IR had a negative correlation with the BD, but it was positively correlated with the TP, CP, NCP, OM, CC, SIC, and root characteristics. The key factors determining soil IIR and SIR were BD, IWC, CP, and CC, and their influencing order was soil BD > CP > IWC > CC. The soil BD was a comprehensive reflection of soil physical properties and was a key direct factor affecting soil IR. Other influencing factors indirectly affected soil IR by changing soil BD. These research findings contribute to a better understanding of the ecological hydrological processes in arid and semi-arid desert regions as well as the water transformation and migration mechanism and its influencing factors under different plant communities, and they are of significance for environmental protection and degraded grassland management. However, future studies should further explore the influencing mechanisms of plant growth and development stage, root structure and type, and distribution characteristics of root biological communities on soil hydrological processes to better understand the effects of soil and plants on water infiltration.

Author Contributions: Writing—original draft S.S. and F.Z.; investigation S.S. and X.W.; methodology, S.S.; formal analysis, X.W.; data curation, Z.M. and X.R.; writing—review and editing, Z.M. and X.R.; supervision, Z.M. and X.D.; All authors have read and agreed to the published version of the manuscript.

Funding: This research was supported by the National Natural Science Foundation of China (42067015), the Natural Science Foundation of Inner Mongolia Autonomous Region (2020MS03038), Desert Ecosystem Conservation and Restoration Innovation Team, and Improvement Innovation Team of Desertification Control.

Data Availability Statement: The datasets generated during and/or analyzed during the current study are available from the corresponding author on reasonable request.

Acknowledgments: We are grateful to the editor for his ability to work on this manuscript during his busy schedule.

Conflicts of Interest: The authors declare that they have no known competing financial interests or personal relationships that could have appeared to influence the work reported in this paper.

References

1. Liu, Z.; Ma, D.; Hu, W.; Li, X.J.S. Land use dependent variation of soil water infiltration characteristics and their scale-specific controls. *Soil Tillage Res.* **2018**, *178*, 139–149. [CrossRef]
2. Liu, Y.; Cui, Z.; Huang, Z.; Lopez-Vicente, M.; Wu, G.L. Influence of soil moisture and plant roots on the soil infiltration capacity at different stages in arid grasslands of China. *Catena* **2019**, *182*, 7. [CrossRef]
3. Bouwer, H. Intake rate: Cylinder infiltrometer. In *Methods of Soil Analysis: Part 1 Physical and Mineralogical Methods*; ASAA and SSSA: Madison, WI, USA, 1986; pp. 825–844.
4. Hillel, D. *Environmental Soil Physics*; Academic Press: San Diego, CA, USA, 1998.
5. Sheng, Q.T.; Dong, L.S. Influence of water quality on soil saturated hydraulic conductivity and infiltration properties. *Trans. Chin. Soc. Agric. Mach.* **2016**, *47*, 108–114. [CrossRef]
6. Cui, Z.; Wu, G.L.; Huang, Z.; Liu, Y. Fine roots determine soil infiltration potential than soil water content in semi-arid grassland soils. *J. Hydrol.* **2019**, *578*, 8. [CrossRef]
7. Wu, G.L.; Yang, Z.; Cui, Z.; Liu, Y.; Fang, N.F.; Shi, Z.H. Mixed artificial grasslands with more roots improved mine soil infiltration capacity. *J. Hydrol.* **2016**, *535*, 54–60. [CrossRef]
8. Gonzalez-Sosa, E.; Braud, I.; Dehotin, J.; Lassabatère, L.; Angulo-Jaramillo, R.; Lagouy, M.; Branger, F.; Jacqueminet, C.; Kermadi, S.; Michel, K. Impact of land use on the hydraulic properties of the topsoil in a small French catchment. *Hydrol. Process.* **2010**, *24*, 2382–2399. [CrossRef]
9. Yu, M.Z.; Zhang, L.L.; Xu, X.X.; Feger, K.H.; Wang, Y.H.; Liu, W.Z.; Schwarzel, K. Impact of land-use changes on soil hydraulic properties of Calcaric Regosols on the Loess Plateau, NW China. *J. Plant Nutr. Soil Sci.* **2015**, *178*, 486–498. [CrossRef]
10. Wang, H.; Zhang, G.H.; Liu, F.; Geng, R.; Wang, L.J. Temporal variations in infiltration properties of biological crusts covered soils on the Loess Plateau of China. *Catena* **2017**, *159*, 115–125. [CrossRef]
11. Luna, L.; Vignozzi, N.; Miralles, I.; Solé-Benet, A. Organic amendments and mulches modify soil porosity and infiltration in semiarid mine soils. *Land Degrad. Dev.* **2018**, *29*, 1019–1030. [CrossRef]
12. Zhu, P.; Zhang, G.; Wang, H.; Xing, S. Soil infiltration properties affected by typical plant communities on steep gully slopes on the Loess Plateau of China. *J. Hydrol.* **2020**, *590*, 125535. [CrossRef]
13. Fischer, C.; Tischer, J.; Roscher, C.; Eisenhauer, N.; Ravenek, J.; Gleixner, G.; Attinger, S.; Jensen, B.; De Kroon, H.; Mommer, L.J.P. Plant species diversity affects infiltration capacity in an experimental grassland through changes in soil properties. *Plant Soil* **2015**, *397*, 1–16. [CrossRef]

14. Chartier, M.P.; Rostagno, C.M.; Pazos, G.E. Effects of soil degradation on infiltration rates in grazed semiarid rangelands of northeastern Patagonia, Argentina. *J. Arid Environ.* **2011**, *75*, 656–661. [CrossRef]
15. Yimer, F.; Messing, I.; Ledin, S.; ABdelkadir, A. Effects of different land use types on infiltration capacity in a catchment in the highlands of Ethiopia. *Soil Use Manag.* **2008**, *24*, 344–349. [CrossRef]
16. Jian, X.L.; Bing, H.H.; Xue, M.M.; Yan, L.L.; Jian, X. Effects of different planting modes on the soil permeability of sloping farmlands in purple soil area. *Chin. J. Appl. Ecol.* **2013**, *24*, 725–731. [CrossRef]
17. Vergani, C.; Graf, F. Soil permeability, aggregate stability and root growth: A pot experiment from a soil bioengineering perspective. *Ecohydrology* **2016**, *9*, 830–842. [CrossRef]
18. Lichner, L.; Holko, L.; Zhukova, N.; Schacht, K.; Rajkai, K.; Fodor, N.; Sándor, R. Plants and biological soil crust influence the hydrophysical parameters and water flow in an aeolian sandy soil. *J. Hydrol. Hydromech.* **2012**, *60*, 309–318. [CrossRef]
19. Xiao, B.; Sun, F.; Hu, K.; Kidron, G. Biocrusts reduce surface soil infiltrability and impede soil water infiltration under tension and ponding conditions in dryland ecosystem. *J. Hydrol.* **2019**, *568*, 792–802. [CrossRef]
20. Eldridge, D.; Greene, R. Microbiotic soil crusts—A review of their roles in soil and ecological processes in the rangelands of Australia. *Soil Res.* **1994**, *32*, 389–415. [CrossRef]
21. Belnap, J.; Welter, J.R.; Grimm, N.B.; Barger, N.; Ludwig, J.A. Linkages between microbial and hydrologic processes in arid and semiarid watersheds. *Ecology* **2005**, *86*, 298–307. [CrossRef]
22. Bu, C.; Wu, S.; Zhang, K.; Yang, Y.; Gao, G. Biological soil crusts: An eco-adaptive biological conservative mechanism and implications for ecological restoration. *Plant Biosyst.* **2015**, *149*, 364–373. [CrossRef]
23. Li, X.R.; Wang, X.P.; Li, T.; Zhang, J.G. Microbiotic soil crust and its effect on vegetation and habitat on artificially stabilized desert dunes in Tengger Desert, North China. *Biol. Fertil. Soils* **2002**, *35*, 147–154. [CrossRef]
24. Wang, X.P.; Li, X.R.; Xiao, H.L.; Berndtsson, R.; Pan, Y.X. Effects of surface characteristics on infiltration patterns in an arid shrub desert. *Hydrol. Process. Int. J.* **2007**, *21*, 72–79. [CrossRef]
25. Xin, Y.; Xie, Y.; Liu, Y.; Liu, H.; Ren, X. Residue cover effects on soil erosion and the infiltration in black soil under simulated rainfall experiments. *J. Hydrol.* **2016**, *543*, 651–658. [CrossRef]
26. Carlesso, R.; Spohr, R.B.; Eltz, F.L.F.; Flores, C.H. Runoff estimation in southern Brazil based on Smith's modified model and the Curve Number method. *Agric. Water Manag.* **2011**, *98*, 1020–1026. [CrossRef]
27. Hao, H.X.; Wei, Y.J.; Cao, D.N.; Guo, Z.L.; Shi, Z.H. Vegetation restoration and fine roots promote soil infiltrability in heavy-textured soils. *Soil Tillage Res.* **2020**, *198*, 104542. [CrossRef]
28. Huang, Z.; Sun, L.; Liu, Y.; Liu, Y.-F.; López-Vicente, M.; Wei, X.-H.; Wu, G.-L. Alfalfa planting significantly improved alpine soil water infiltrability in the Qinghai-Tibetan Plateau. *Agric. Ecosyst. Environ.* **2019**, *285*, 106606. [CrossRef]
29. Archer, N.; Quinton, J.N.; Hess, T. Below-ground relationships of soil texture, roots and hydraulic conductivity in two-phase mosaic vegetation in South-east Spain. *J. Arid Environ.* **2002**, *52*, 535–553. [CrossRef]
30. Leung, A.K.; Garg, A.; Coo, J.L.; Ng, C.W.W.; Hau, B. Effects of the roots of *Cynodon dactylon* and *Schefflera heptaphylla* on water infiltration rate and soil hydraulic conductivity. *Hydrol. Process.* **2015**, *29*, 3342–3354. [CrossRef]
31. Meng, Z.; Dang, X.; Gao, Y.; Ren, X.; Ding, Y.; Wang, M. Interactive effects of wind speed, vegetation coverage and soil moisture in controlling wind erosion in a temperate desert steppe, Inner Mongolia of China. *J. Arid Land* **2018**, *10*, 534–547. [CrossRef]
32. Institute of Soil Science, Chinese Academy of Sciences. *Determination of Soil Physical Properties*; China Science Publishing & Media Ltd.: Beijing, China, 1978.
33. Horton, R.E. An Approach toward a Physical Interpretation of Infiltration-Capacity. *Soil Sci. Soc. Am. J.* **1941**, *5*, 399–417. [CrossRef]
34. Green, W.H.; Ampt, G.A. Studies on Soil Phyics. *J. Agric. Sci.* **1911**, *4*, 1–24. [CrossRef]
35. Wang, J.; Watts, D.B.; Meng, Q.Q.; Zhang, Q.F.; Way, T.R. Influence of Surface Crusting on Infiltration of a Loess Plateau Soil. *Soil Sci. Soc. Am. J.* **2016**, *80*, 683–692. [CrossRef]
36. Zhang, J.; Lei, T.W.; Qu, L.Q.; Chen, P.; Gao, X.F.; Chen, C.; Yuan, L.L.; Zhang, M.L.; Su, G.X. Method to measure soil matrix infiltration in forest soil. *J. Hydrol.* **2017**, *552*, 241–248. [CrossRef]
37. Kabir, E.B.; Bashari, H.; Bassiri, M.; Mosaddeghi, M.R. Effects of land-use/cover change on soil hydraulic properties and pore characteristics in a semi-arid region of central Iran. *Soil Tillage Res.* **2020**, *197*, 104478. [CrossRef]
38. Hu, W.; Shao, M.; Wang, Q.; Fan, J.; Horton, R. Temporal changes of soil hydraulic properties under different land uses. *Geoderma* **2009**, *149*, 355–366. [CrossRef]
39. Jarvis, N.; Koestel, J.; Messing, I.; Moeys, J.; Lindahl, A. Influence of soil, land use and climatic factors on the hydraulic conductivity of soil. *Hydrol. Earth Syst. Sci.* **2013**, *17*, 5185–5195. [CrossRef]
40. Bodner, G.; Leitner, D.; Kaul, H.-P. Coarse and fine root plants affect pore size distributions differently. *Plant Soil* **2014**, *380*, 133–151. [CrossRef]
41. Kalhoro, S.A.; Ding, K.; Zhang, B.Y.; Chen, W.Y.; Hua, R.; Shar, A.H.; Xu, X.X. Soil infiltration rate of forestland and grassland over different vegetation restoration periods at Loess Plateau in northern hilly areas of China. *Landsc. Ecol. Eng.* **2019**, *15*, 91–99. [CrossRef]
42. Castellano, M.J.; Valone, T.J. Livestock, soil compaction and water infiltration rate: Evaluating a potential desertification recovery mechanism. *J. Arid Environ.* **2007**, *71*, 97–108. [CrossRef]

43. Benavides, I.F.; Solarte, M.E.; Pabon, V.; Ordonez, A.; Beltran, E.; Rosero, S.; Torres, C. The variation of infiltration rates and physical-chemical soil properties across a land cover and land use gradient in a Paramo of southwestern Colombia. *J. Soil Water Conserv.* **2018**, *73*, 400–410. [CrossRef]
44. Azooz, R.H.; Arshad, M.A. Soil infiltration and hydraulic conductivity under long-term no-tillage and conventional tillage systems. *Can. J. Soil Sci.* **1996**, *76*, 143–152. [CrossRef]
45. He, F.H.; Pan, Y.H.; Tan, L.L.; Zhang, Z.H.; Li, P.; Liu, J.; Ji, S.X.; Qin, Z.H.; Shao, H.B.; Song, X.Y. Study of the water transportation characteristics of marsh saline soil in the Yellow River Delta. *Sci. Total Environ.* **2017**, *574*, 716–723. [CrossRef] [PubMed]
46. Liu, H.; Lei, T.; Zhao, J.; Yuan, C.; Fan, Y.; Qu, L. Effects of rainfall intensity and antecedent soil water content on soil infiltrability under rainfall conditions using the run off-on-out method. *J. Hydrol.* **2011**, *396*, 24–32. [CrossRef]
47. Ghestem, M.; Sidle, R.C.; Stokes, A. The influence of plant root systems on subsurface flow: Implications for slope stability. *Bioscience* **2011**, *61*, 869–879. [CrossRef]
48. Zhao, Y.G.; Wu, P.T.; Zhao, S.W.; Feng, H. Variation of soil infiltrability across a 79-year chronosequence of naturally restored grassland on the Loess Plateau, China. *J. Hydrol.* **2013**, *504*, 94–103. [CrossRef]
49. Leung, A.K.; Boldrin, D.; Liang, T.; Wu, Z.; Kamchoom, V.; Bengough, A. Plant age effects on soil infiltration rate during early plant establishment. *Géotechnique* **2018**, *68*, 646–652. [CrossRef]
50. Fischer, C.; Roscher, C.; Jensen, B.; Eisenhauer, N.; Baade, J.; Attinger, S.; Scheu, S.; Weisser, W.W.; Schumacher, J.; Hildebrandt, A. How do earthworms, soil texture and plant composition affect infiltration along an experimental plant diversity gradient in grassland? *PLoS ONE* **2014**, *9*, e98987. [CrossRef]
51. Logsdon, S.D.; Allmaras, R.R. Maize and soybean root clustering as indicated by root mapping. *Plant Soil* **1991**, *131*, 169–176. [CrossRef]
52. Wu, G.L.; Cui, Z.; Huang, Z. Contribution of root decay process on soil infiltration capacity and soil water replenishment of planted forestland in semi-arid regions. *Geoderma* **2021**, *404*, 115289. [CrossRef]
53. Huang, Z.; Tian, F.P.; Wu, G.L.; Liu, Y.; Dang, Z.Q. Legume grasslands promote precipitation infiltration better than gramineous grasslands in arid regions. *Land Degrad. Dev.* **2017**, *28*, 309–316. [CrossRef]
54. Bronick, C.J.; Lal, R. Soil structure and management: A review. *Geoderma* **2005**, *124*, 3–22. [CrossRef]
55. Zhang, G.H.; Xie, Z.F. Soil surface roughness decay under different topographic conditions. *Soil Tillage Res.* **2019**, *187*, 92–101. [CrossRef]
56. Lipiec, J.; Kus, J.; Slowinska-Jurkiewicz, A.; Nosalewicz, A. Soil porosity and water infiltration as influenced by tillage methods. *Soil Tillage Res.* **2006**, *89*, 210–220. [CrossRef]